



# Optical properties of oxidized single-wall carbon nanotubes



M. Ohfuchi<sup>a,\*</sup>, Y. Miyamoto<sup>b</sup>

<sup>a</sup> Fujitsu Laboratories Ltd., Atsugi, 243-0197, Japan

<sup>b</sup> Research Center for Computational Design of Advanced Functional Materials, National Institute of Advanced Industrial Science and Technology (AIST), Tsukuba, 305-8568, Japan

## ARTICLE INFO

### Article history:

Received 29 June 2016

Received in revised form

5 December 2016

Accepted 18 December 2016

Available online 19 December 2016

## ABSTRACT

Optical properties of oxidized single-wall carbon nanotubes (SWCNTs) have attracted much attention because of the greater luminescence quantum yield than that of pristine CNTs, showing the possibility of optical applications such as near-infrared single-photon emitters and bioimaging. To advance the fundamental understanding of the optical properties, we theoretically investigated the energetics and the optical transitions for complex oxygen (O) adsorption structures on (6,5) CNTs, including adsorption of two O atoms. For CNTs adsorbed by isolated O atoms, four groups of optical transition levels were obtained below  $E_{11}$ . We also found two additional groups of optical transition levels for adsorption structures of two O atoms, whose related adsorption structures are more stable than the isolated O-adsorption structures. These results explain the multiple emission peaks and their irradiation time dependence in the photoluminescence (PL) spectra for CNTs oxidized by ultraviolet ozone, providing a possible mechanism for significant brightening of the emission whose wavelength range is ideal for biological imaging. Our results are also consistent with the PL measurements of SWCNTs oxidized by  $O_2$  molecules during single chirality separation processes. This comprehensive understanding is essential for further applications of oxidized SWCNTs.

© 2016 Elsevier Ltd. All rights reserved.

## 1. Introduction

Introduction of oxygen (O) atoms to single-wall carbon nanotubes (SWCNTs) at low concentrations drastically changes their optical properties [1,2]. When SWCNTs are exposed to ozone ( $O_3$ ) and light, a new distinct emission red-shifted from the  $E_{11}$  peak increases its intensity in process of time. The red-shifted emission is represented like  $E_{11}^*$ . This controllable treatment is called oxygen doping by analogy to doping of semiconductor materials. Mobile excitons generated in undoped nanotube regions are trapped at oxygen sites when they migrate to doped regions and provide strong red-shifted luminescence before non-radiative decay due to collisions between mobile excitons, quenching at defects and end sites of CNTs, and so on [1,2]. It has been reported, however, that intrinsic non-radiative decay paths, i.e. dark states, still lie below the  $E_{11}^*$  level [2]. A significant brightening of  $E_{11}^*$  emission has been demonstrated by creating an optically allowed state below the dark states with another type of adsorbate called diazonium [3]. Other

adsorbates have also been used to create red-shifted emission; dialkylation [4] and aminoaryl groups [5]. These red-shifted emissions suggest potential application of SWCNTs for novel photonic devices such as near-infrared single-photon emitters [6] and bioimaging [1,5].

The emission mechanism has also been intensively investigated [7–9]. Low-temperature photoluminescence (PL) experiments have revealed that the  $E_{11}^*$  level splits into three ( $E_{11}^{*+}$ ,  $E_{11}^*$ , and  $E_{11}^{*-}$ ), and computational simulations have assigned different adsorption structures of an O atom with the electronic structures corresponding to these peaks [7]. In this study, we investigate complex O-adsorption structures produced during the  $O_3$  oxidation process of SWCNTs and their optical properties toward a more comprehensive understanding, including adsorption structures of two O atoms. We also aim to explain the recent bioimaging experiments where the  $E_{11}^{*-}$  emission increases its intensity with respect to  $E_{11}^*$  as the ultraviolet (UV)/ozone irradiation time increases [10]. The wavelength range of  $E_{11}^{*-}$  is ideal for biological imaging. We use (6,5) CNTs for our calculations because most of the experiments have been conducted using CNTs with this chirality.

\* Corresponding author.

E-mail address: [mari.ohfuti@jp.fujitsu.com](mailto:mari.ohfuti@jp.fujitsu.com) (M. Ohfuchi).

## 2. Computational methods

The stable geometry of the O-adsorption structures and the reaction paths are examined using the density functional theory (DFT) code OpenMX [11–13]. This code uses pseudoatomic orbitals (PAOs) [11] as the basis function set. The exchange–correlation potential was treated with the Perdew–Burke–Ernzerhof generalized gradient approximation (GGA–PBE) [14]. The electron–ion interaction was described by norm-conserving pseudopotentials [15] with partial core correction [16]. We used the PAOs specified by C-s2p2d1 and O-s2p2d1, where C and O are atomic symbols for carbon and oxygen, respectively, and s2, for example, indicates the employment of two orbitals for the s component. For both atomic species, 7.0 Bohr was chosen as the cutoff radii of the PAOs. The energy band occupation was smeared by the Fermi distribution function (the temperature  $T = 300$  K) to perform stable self-consistent calculations. The unit cell of (6,5) carbon nanotubes (CNTs) has 364 atoms. A periodic boundary condition was applied and three  $k$  points were used for the reciprocal space integration. The atomic structure was fully relaxed using a 3 nm-square lateral unit cell, and the optimum unit length was determined. We model O atoms with low concentrations by placing one or two atoms in the unit cell. The geometry optimization of CNTs adsorbed with O atoms was executed while maintaining the unit length of the CNTs. In addition, the reaction path was investigated using the nudged elastic band (NEB) method [17]. The spring constant for the NEB method was set to be  $970 \text{ eV/nm}^2$ . The dissociation path of  $\text{O}_2$  from ozonides was determined using the NEB method in the spin-unrestricted formalism [18–20]. The convergence criterion of forces on atoms was set to 0.1 and 0.5 eV/nm for geometry optimization and reaction path calculations, respectively.

For the calculations of the optical transitions, we used finite-length CNTs with the edges terminated by hydrogen (H) atoms [21–25]. The optimized geometry was also determined using OpenMX as described in the previous paragraph. The optical transition energies and the oscillator strengths were calculated with finite-length models of CNTs, using time-dependent DFT (TDDFT) with B3LYP functional as implemented in the Gaussian 09 program [26]. Validation of using TDDFT for optical transition properties was discussed in Ref. [27]. As discussed in Ref. [27], the TDDFT optical excitation can include excitonic effect approximately if the model is finite. When the finite-length model for nanotube is used and if the length is beyond the wave function extension of exciton, the computed optical spectroscopy obtained by TDDFT shows reasonable agreement to experiments [25]. We used 10 nm-long CNTs and a 3-21G orbital set, which give the converged results in the present computational scheme, i.e. TDDFT with B3LYP functional (see Supplementary Data, 1). The structure of (6,5) CNTs includes 892 C atoms. These methods have been successfully used to describe the oxidation of SWCNTs [28,29] and their optical properties [7,9,21–24].

## 3. Results and discussion

### 3.1. $\text{O}_3$ oxidation process

Fig. 1 shows the definition of bonds “a”, “b”, and “c” in CNTs and the schematic diagrams of adsorption structures of O atoms. We start with three ozonides—ozonide-a, ozonide-b, and ozonide-c—where the ozonide structure is formed on bonds “a”, “b”, and “c”, respectively. Throughout this paper, the adsorption (formation) energy is defined as  $E_{\text{ad}} = E(\text{CNT} + N_{\text{O}}\text{O}) - E(\text{CNT}) - N_{\text{O}}/2 E(\text{O}_2)$ , where  $N_{\text{O}}$  is the number of O atoms,  $E(\text{CNT} + N_{\text{O}}\text{O})$  is the total energy of the CNTs adsorbed with O atoms, and  $E(\text{CNT})$  and  $E(\text{O}_2)$  are those of the CNTs and  $\text{O}_2$ , respectively. The three ozonides have

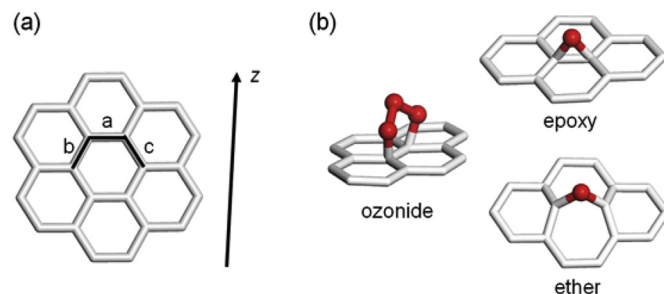


**Fig. 1.** (a) Definition of bonds “a”, “b”, and “c”. The nanotube axis in the  $z$ -direction is indicated by an arrow. (b) Schematic diagrams of oxygen (O)-adsorption structures. The gray sticks and red spheres represent C–C bonds and O atoms, respectively. (A colour version of this figure can be viewed online.)

almost the same O-adsorption energy; the values are 13.1, 14.6, and 13.1 kcal/mol for ozonide-a, ozonide-b, and ozonide-c, respectively. Considering that the formation energy of  $\text{O}_3$  is 32.4 kcal/mol, the ozonides are easily formed on the (6,5) nanotubes. Fig. 2a–c show the reaction barrier for some dissociation processes of  $\text{O}_2$  from ozonides on (6,5) nanotubes. The reaction barrier of dissociation of  $\text{O}_2$  from ozonides is approximately 10 kcal/mol for all cases, meaning that dissociation is very likely to occur under room temperature. Thus isolated O atoms are left on the CNTs. The O atom forms an ether structure on bond “a”, or epoxy structure on bonds “b” or “c” [1,28,30]. Fig. 2d–f show the energy barriers when O atoms move to neighboring sites. The O atom forming the ether-a structure faces energy barriers of more than 40 kcal/mol, meaning that the O atom remains in its position. On the other hand, the energy barrier of epoxy-b and epoxy-c structures moving to neighboring sites is moderate, approximately 20 kcal/mol. The O atoms forming epoxy-b and epoxy-c structures move along the tube axis (see Fig. 1a) or are trapped in ether-a structures. For the isolated O atoms, many more ether-a structures exist on the surface of CNTs than epoxy structures. Although we should consider the dynamics under each experimental condition, the equilibrium ratio of the ether-a structures to the epoxy structures is estimated to be  $10^{14}$  from their adsorption energies.

### 3.2. Optical properties of (6,5) CNTs adsorbed by isolated O atoms

Here we discuss the optical properties of (6,5) CNTs adsorbed by isolated O atoms. Fig. 3 shows the optical transition energy and the oscillator strength of pristine and O-adsorbed CNTs. The pristine nanotube shows a large peak at 1.38 eV, which corresponds to the  $E_{11}$  level, showing a good agreement with the experimental value, 1.27 eV [31]. The data of O-adsorbed CNTs are superimposed in Fig. 3a. The optical properties of isolated O-adsorbed (6,5) CNTs have also reported in Ref. [7]. Our results for the ether-a and epoxy-b structures agree with those in Ref. [7]. In addition to these two structures, we examined the epoxy-c structure. We consider that the epoxy-c structure should be included to describe the optical properties of O-adsorbed (6,5) CNTs because it has the lower adsorption energy than the ether structure parallel to the tube axis that has been mentioned as ether-I structure in Ref. [7]. As shown in Fig. 3a, the  $E_{11}$  peak is split into several peaks, which has been discussed as  $E_{11}^+$  and  $E_{11}^-$  in Ref. [7]. The  $E_{11}^+$  peak is described by the ether-I structure in Ref. [7]; however the epoxy-c structure produces the peak in our results. The ether-a structure has a peak at 1.29 eV, 0.1 eV below  $E_{11}$ , which is well known as  $E_{11}^*$  [1]. The degenerated  $E_{11}$  levels of pristine nanotubes are split upon O-adsorption and produce an optically allowed state with a lower energy. We found that the epoxy-c structure produces a peak at the

Download English Version:

<https://daneshyari.com/en/article/5432530>

Download Persian Version:

<https://daneshyari.com/article/5432530>

[Daneshyari.com](https://daneshyari.com)